Cerebral Cortex Advance Access published March 28, 2004

Temporal Envelope Processing in the Human Left and Right Auditory Cortices

Catherine Liégeois-Chauvel[1], Christian Lorenzi[2], Agnès Trébuchon[1], Jean Régis[1] and Patrick Chauvel[1]

[1]INSERM EMI-U 99-26. Laboratoire de Neurophysiologie et Neuropsychologie, Marseille, France and [2]Laboratoire de Psychologie Expérimentale, UMR CNRS 8581, Université René Descartes Paris 5, 71 avenue Edouard Vaillant, 92774 Boulogne-Billancourt Cédex, France, & Institut Universitaire de France

The goal of this study was to determine the temporal response properties of different auditory cortical areas in humans. This is achieved by recording the phase-locked neural activity to white noises modulated sinusoidally in amplitude (AM) at frequencies between 4 and 128 Hz, in the left and right cortices of 20 subjects. Phase-locked neural responses are recorded in four auditory cortical areas with intracerebral electrodes, and modulation transfer functions (MTFs) are computed from these responses. A number of MTFs are bandpass in shape, demonstrating a selective encoding of AM frequencies below 64 Hz in the auditory cortex. This result provides strong physiological support to the idea that the human auditory system decomposes the temporal envelope of sounds (such as speech) into its constituting AM components. Moreover, the results show a predominant response of cortical auditory areas to the lowest AM frequencies (4–16 Hz). This range matches the range of AM frequencies crucial for speech intelligibility, emphasizing therefore the role played by these initial stations of cortical processing in the analysis of speech. Finally, the results show differences in AM sensitivity across cortical areas and hemispheres, and provide a physiological foundation for claims of functional specialization of auditory areas based on previous population measures.

Keywords: amplitude modulation, auditory cortex, hearing, human, synchronization, temporal envelope

Introduction

Most species-specific vocalizations show prominent temporal-envelope fluctuations (i.e. amplitude modulations or AM) in the low frequency range (<100 Hz; e.g. Kaltwasser, 1990). By comparison, speech shows prominent AM in the frequency range of 2–16 Hz, with a maximum at 3–4 Hz that corresponds to the average syllabic rate (Steeneken and Houtgast, 1980). In humans, psychophysical studies have demonstrated that AM frequencies crucial for speech intelligibility range from 4–16 Hz (e.g. Drullman *et al.*, 1994a,b; Shannon *et al.*, 1995; Smith *et al.*, 2002). Consistent with these studies, neuropsychological data have shown that a loss of sensitivity in this low AM frequency range is associated with speech and language disorders (Hescot *et al.*, 2000; Lorenzi *et al.*, 2000; Rocheron *et al.*, 2002; Witton *et al.*, 2002).

In non-human species, the capacity of single auditory neurons to encode these temporal-envelope fluctuations is often assessed by measuring modulation transfer functions (MTFs) showing neural synchronization to the stimulus envelope or mean firing rate as a function of the stimulus AM frequency (the maximum of an MTF with bandpass shape is called 'best' modulation frequency or BMF). Most electrophysiological studies based on MTF measurements in mammals have provided evidence that the ability of auditory neurons to encode the envelope of AM sounds deteriorates with increasing level of the auditory system, i.e. the mean BMF of auditory neurons decreases from the auditory nerve to the auditory cortex (Langner, 1992; Frisina, 2001). Therefore, only the lowest AM frequencies (<30 Hz) are preserved at the cortical level. Moreover, as suggested below, these low AM frequencies are encoded differentially in primary and secondary cortical areas, suggesting the existence of functional cortical maps in the temporal domain.

Most studies have shown that a number of sub-cortical and cortical neurons sensitive to envelope fluctuations display a characteristic bandpass MTF shape, and respond therefore by tuning to a certain BMF (e.g. Schreiner and Urbas, 1986, 1988; Eggermont, 1994). Such a tuning property may reflect an important aspect of auditory processing, because it suggests that the central auditory system decomposes the envelope of sounds into its AM components.

Differences in the organization of these tuning properties (i.e. differences in BMF values) between auditory cortical areas have been reported in various species (Schreiner and Urbas, 1986, 1988; Bieser and Müller-Preuss, 1996). However, no clear organized topography of these selectivities to low AM frequencies could be determined within cortical areas. A topographical organization of these tuning properties has been found in the inferior colliculus and primary auditory cortex of mammals. Yet, in each case, this organization was found for high AM frequencies only (>50 Hz) and cortical tuning was observed in terms of firing rate instead of phase-locking (Schulze and Langner, 1997; Schulze *et al.*, 2002).

Although there is a considerable amount of data on AM coding in animals, little is known about (i) the organization of temporal resolution between and within cortical auditory areas in humans and (ii) how this organization relates to speech perception. A correlation between the steady-state potentials evoked from the scalp of human listeners in response to AM sounds and the perceptual MTF (e.g. Viemeister, 1979) was obtained in an electroencephalography (EEG) study conducted by Rees *et al.* (1986). In this study, sounds were modulated at frequencies ranging from 5 to 400 Hz. A magnetoencephalography (MEG) study also showed that the primary auditory cortex responds to AM frequencies ranging from 10 to 100 Hz (Roß *et al.*, 2000). As in the EEG study of Rees *et al.* (1986), the steady-state evoked magnetic fields detected from human listeners correlated well with the perceptual MTF. Another MEG study using complex tones (Langner *et al.*, 1997) suggested the existence of a topographical organization in the human auditory cortex for high AM frequencies (from 50 to 400 Hz). However, the AM frequencies used in both MEG studies were much higher than those known to generate the best cortical response (e.g. Schreiner and Urbas, 1988). More-

over, AM frequencies >10–50 Hz appear less crucial to speech perception than low ones (4–16 Hz), as degradations in these high AM frequencies do not affect speech intelligibility (e.g. Drullman *et al.*, 1994a,b). This is emphasized by the results of a recent MEG study demonstrating that the match between the speech rate and the capacities of the human auditory cortex to follow AM is a prerequisite for speech intelligibility (Ahissar *et al.*, 2001).

A functional magnetic resonance imaging (fMRI) study (Giraud *et al.*, 2000) also investigated the cortical representation of AM using a set of white noises modulated sinusoidally in amplitude at frequencies covering a broad range (4–256 Hz). Consistent with animal studies, this study revealed that, in humans: (i) temporal resolution degrades from the brainstem to the auditory cortex and (ii) most cortical regions were tuned to low AM frequencies (4–8 Hz) and only a few to high AM frequencies. However, unlike in the study of Langner *et al.* (1997), no clear topographical organization of these AM selectivities was observed between and within cortical areas.

The high spatial resolution of the fMRI technique is well-suited to the production of cortical maps in human, but its poor temporal resolution limits the investigation of the phase-locked cortical response to AM. On the other hand, the EEG and MEG techniques have better temporal resolution, but provide insufficient spatial information regarding the localization of the various cortical areas involved in AM coding. Presurgical investigation of patients being candidates for cortectomy for the relief of intractable epilepsy allows direct recording from the cerebral cortex. This so-called SEEG (for stereo-electro-encephalography) technique is based on recording from multiple electrodes implanted in different cortical structures, in order to determine which structures are involved in the initiation and propagation of seizures (e.g. Bancaud *et al.*, 1965). The results of previous studies (Liégeois-Chauvel *et al.*, 1991, 1994) have shown that four auditory areas can be identified from the morphological distribution of auditory evoked potentials (AEPs) within the superior temporal gyrus (STG): (i) the primary auditory cortex (PAC), located in the medial and intermediate part of Heschl's gyrus (HG); (ii) the secondary auditory cortex (SAC), located in the lateral part of HG and the planum temporale (PT); (iii) an area located in the posterior part of STG (Post T1); and (iv) an area located in front of HG, in the anterior part of STG (BA 22). The SEEG technique provides therefore a unique opportunity to: (i) localize the human cortical areas producing a phase-locked response to AM; (ii) assess whether or not in humans, cortical neurons show tuning properties in the temporal domain; and (iii) investigate the organization of such tuning properties between and within areas. To address these issues, the response properties of the four areas described above were determined in the left and right human cortices, by recording the phase-locked neural response to AM sounds '*in vivo*' and computing 'neural' MTFs from these responses.

Material and Methods

Subjects

Twenty epileptic patients (eight males, 12 females, 18–50 years of age) participated in this study. They suffered from drug-resistant partial epilepsy and were implanted with chronic SEEG electrodes in the right (nine patients) or left auditory cortex (11 patients) (i.e. HG, PT, Post T1 and BA 22). Several additional electrodes were implanted in various cortical structures in order to: (i) determine which ones were involved in the initiation and propagation of seizures and (ii) delineate accurately the limits of future cortical excision (Talairach *et al.*, 1974). The choice of the anatomical location of electrodes was based on clinical and video-EEG recordings and MRI, and was made independently of the present study. It is important to note that these patients were selected a posteriori in such a way that, in 19 out of the 20 patients, the epileptogenic zone did not involve auditory areas. In the remaining patient, HG corresponded to the epileptogenic zone and the electrode implanted in BA 22 was only considered in the present study. Neuropsychological assessment indicated that all patients showed typical language representation. Recordings of brainstem evoked potentials and pure-tone audiograms carried out before SEEG indicated intact cochlear and brainstem auditory functions.

This study did not add any invasive procedure to the depth EEG recordings performed routinely in the neurological evaluation. All patients were informed about the research protocol during SEEG and gave their fully informed consent for participating in this study.

Anatomical Definition of Depth Electrode Position

The stereotactic method was based on the co-registration of the patient's MRI with the stereotactic angiogram. This was performed in order to avoid any injury of brain vessels. Moreover, this method allowed orthogonal introduction of multilead electrodes (0.8 mm diameter, 10 or 15 electrode contacts of 2 mm length, each with 1.5 mm spacing between contacts) in the stereotactic space (Szikla *et al.*, 1977; Talairach and Tournoux, 1988). The anatomical position of each contact was then identified on the basis of (i) an axial scanner image acquired before the removal of electrodes and (ii) an MRI scan performed after the removal of electrodes (Liégeois-Chauvel *et al.*, 1991).

Figure 1 shows two examples of intracerebral electrodes located in the right (Case 3) and left (Case 7) auditory cortices. In Case 3, the medial contacts (1–4) of electrode P recorded from the medial part of the right HG (that is PAC) whereas the lateral contacts (5–9) recorded activity from PT. Contacts 3–5 of electrode T were located in the lateral part of HG, that is in SAC, whereas the lateral contacts (6–9) were in BA 22. Contacts 3–6 of electrode H were located in PAC, whereas contacts 7–8 were in PT. In Case 7, four contacts of electrode H′ were in left PAC and four contacts were in left SAC.

Table 1 presents the location of the 162 electrode contacts recording auditory evoked potentials (AEPs) from different auditory cortical areas for the 20 patients (labelled C1–C20). Each cell of Table 1 shows the number of electrode contacts located in a given area for each patient. The last line indicates the number of electrode contacts within each auditory area across patients: 65 contacts recorded

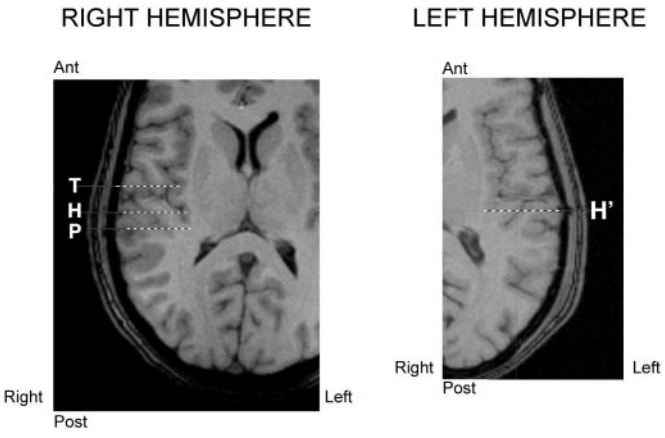

Figure 1. Two examples of intracerebral electrodes localized in the right (Case 3) and left (Case 7) auditory cortices superimposed on the patients MRI slices. In both images, each dashed line (labeled T, H, H′ and P) indicates the anatomical location of a single electrode (each white segment corresponding to a given electrode contact). Contacts are labeled from 1 (for the most medial contact) to 10 (for the most lateral contact). The anatomical position of each contact is described in the text (Materials and Methods).

Table 1
Location of the 162 contacts recording auditory evoked potentials (AEPs) from different cortical areas for the 20 patients (labelled C1–C20)

PAC		SAC		Post-T1		BA 22	
Left	Right	Left	Right	Left	Right	Left	Right
C7: 4	C1: 5	C7: 4	C14: 5	C8: 4	C1: 8	C10: 4	C3: 4
C8: 3	C2: 3	C11: 5	C3: 10	C9: 3	C2: 4	C19: 4	C17: 6
C9: 2	C3: 8	C12: 4	C5: 5	C10: 2	C4: 3		C18: 5
C12: 3	C4: 6	C15: 4			C6: 3		
C11: 3	C6: 5	C16: 2		C13: 2			
C12: 5				C15: 3			
C13: 3							
C14: 3							
C20: 12							
38 leads	27 leads	19 leads	20 leads	17 leads	18 leads	8 leads	15 leads

activity in PAC (27 and 38 leads in the right and left cortices, respectively); 39 contacts were located in SAC (20 and 19 leads in the right and left cortices, respectively); 35 contacts were located in Post T1 (18 and 17 leads in the right and left cortices, respectively); and 23 contacts were located in BA 22 (15 and 18 leads in the right and left cortices, respectively).

Automatic segmentation of the cerebral cortex and analysis of individual variations in the patient anatomy (sulcal pattern) were also conducted using an original software ('Anatomist'; Mangin *et al.*, 1995). In Figure 2, the 3D display of the auditory structures of STG [HG (red); PT (dark blue), BA 22 (purple) and Post T1 (brown)] and insula (light blue) shows the anatomical location of the four auditory areas listed in Table 1. PAC is physiologically located in the postero-dorso-medial part of HG (Liégeois-Chauvel *et al.*, 1991) and SAC encompasses the lateral part of HG and PT (Liégeois-Chauvel *et al.*, 1994).

Stimuli

All stimuli were generated using a 16-bit D/A converter at a sampling frequency of 44.1 kHz. The stimuli were white noises modulated sinusoidally in amplitude at frequencies *fm* of 4, 8, 16, 32, 64 and 128 Hz, with a modulation depth of 100 %. The starting phase of the modulation was fixed at 270° (thus, each stimulus started at an amplitude minimum in the modulation waveform). All AM stimuli were 1 s in duration and were shaped by rising and falling 25 ms cosine ramps/damps. They were equated in rms (root mean square) and presented binaurally via Sennheiser headphones at 75 dB SPL (rms). Series of 100 mixed stimuli (128/16 Hz; 4/32 Hz, 8/64 Hz) were delivered to each listener in random order.

Unlike the MEG studies cited above, white-noise carriers were used in order to avoid the influence of any spectral cues such as spectral sidebands (the modulation of white noise does not affect its (flat) long-term power spectrum) or distortion products in the audio-frequency domain (it is noteworthy that many electrophysiological studies cited in the Introduction did not attempt to mask these distortion products, knowing that the frequency of distortion products generated by the cochlea may be equal to the modulation frequency).

Recordings

The recordings of intracerebral AEPs were monopolar, with each contact of a given depth electrode referenced to an extra-dural lead. All signals were amplified and bandpass filtered between 0.15 and 200 Hz [more precisely, a highpass filter (cutoff frequency, 0.15 Hz; rolloff, 12 dB/oct) and a lowpass filter (cutoff frequency, 200 Hz; rolloff, 24 dB/oct) were used to bandpass filter signals]. Data acquisition started 164 ms before the presentation of the sound and lasted for 1476 ms. During each recording session, the patient laid comfortably in a chair in a sound-attenuated room and listened passively to the sounds.

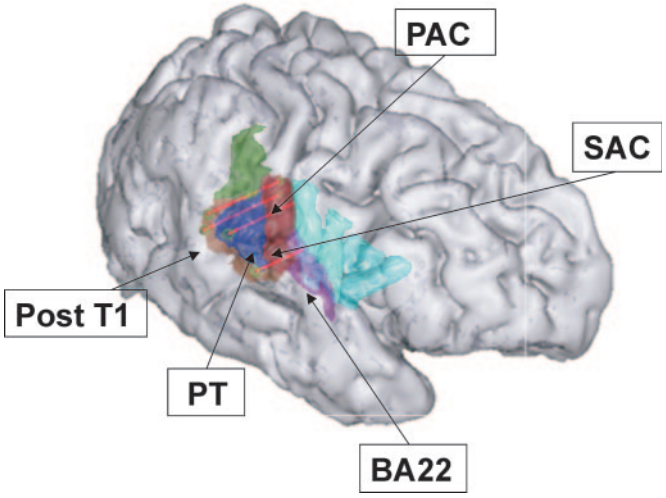

Figure 2. Anatomical location of the auditory structures of STG [HG (red); PT (dark blue), BA 22 (purple) and post T1 (brown)] and insula (light blue) listed in Table 1. Area Post T1 corresponds to the posterior part of STG and area BA 22 corresponds to the anterior part of STG (also called Ant T1).

Data Analysis

The magnitude of the evoked response (averaged over 50 trials) was analyzed as a function of the stimulus modulation frequency, *fm*. The magnitude values of the components at this stimulus modulation frequency were determined by taking the fast Fourier transform of the averaged responses and local field potential (*lfp*) MTFs – conceptually identical to those reported previously in EEG studies (e.g. Rees *et al.*, 1986), electrophysiological studies (e.g. Schreiner and Urbas, 1986, 1988), or psychoacoustical studies (e.g. Viemeister, 1979) – were then computed for each contact. For a given subject and a given electrode, each magnitude (in μV) was divided by the maximum magnitude value observed across electrode contacts. Therefore, each *lfp*-MTF shows the normalized magnitude of the response evoked by AM (ranging from 0–1) as a function of stimulus AM frequency (in Hz). In the present study, the maximum of an MTF with bandpass shape is called 'best' modulation frequency or BMF, and the maximum of an MTF with lowpass shape is called 'corner' modulation frequency or CMF.

Results

General Patterns of Evoked Responses Driven by AM Sounds

Auditory evoked responses reflecting AM coding were recorded in different areas of the auditory cortex. Two types of evoked responses were observed: (i) some AEPs followed the stimulus' temporal envelope and showed better synchronization to either one or two AM periods and (ii) other AEPs displayed simple on and off responses and failed to follow the stimulus' temporal envelope (an example is provided in Fig. 4 for the region of SAC). These two types of AEPs were recorded in each auditory cortical area. Overall, synchronized AEPs and AEPs displaying simple on/off responses were observed in 74 and 26% of all recording sites, respectively.

Analysis of the Synchronized AEPs

Figure 3 (left panel: *A*, *B*, *C*) shows typical synchronized AEPs recorded from three different sites of the auditory cortex together with the corresponding *lfp*-MTFs (right panels) computed from these AEPs (cf. Data Analysis section). Each AEP plot shows the amplitude of the evoked responses (in μV) as a function of time (in ms). For each MTF plot, the ordinate shows the amplitude of the evoked response (normalized by the maximum value across contacts for the electrode under study) as a function of the stimulus modulation frequency, *fm*. For each recording location, only the AEP with the highest local synchrony is illustrated [in the present example, highest synchrony is obtained at *fm* = 4 Hz (upper graph: *A*), 8 Hz (middle graph: *B*) and 16 Hz (lower graph: *C*)]. Periodic activity characterized by phasic responses close to the onset of each modulation cycle is clearly visible in these averaged AEPs. It is manifested as a maximum (i.e. a CMF or BMF) at 4, 8 or 16 Hz in the corresponding *lfp*-MTF. For instance, for recording site A, the time-interval between successive peaks of the AEP cycle is ~245 ms (which corresponds to the 250 ms period of the AM stimulus). For recording site B, this time-interval is ~122 ms (which corresponds to the 125 ms period of the AM stimulus). Responses evoked by other AM noises at the same cortical location display little periodic activity as shown by the computed *lfp*-MTF. Periodic activity strongly phase-locked to the stimulus envelope is also observed in the averaged AEP recorded from site C when *fm* = 16 Hz.

Figure 4 presents similar AEPs recorded in the anterior PAC, posterior PAC and SAC in response to a 32 Hz AM. In the anterior part of PAC, neural activity appears to be strongly phase-locked to the 32 Hz AM. By contrast, a weak response is recorded from the contact located in posterior PAC where best synchronization is observed for a 8 Hz AM (as shown by the computed *lfp*-MTF; upper panel) and no periodic response is observed in the region of SAC presented here. These data suggest therefore the existence of a spatial difference in the AM frequency range of phase-locking within PAC.

Different MTF Shapes in the Auditory Cortex

Figure 5 displays the different types of *lfp*-MTF observed in cortical auditory areas. Some *lfp*-MTFs show a maximum below 4–8 Hz (top row), resulting in a lowpass shape given the

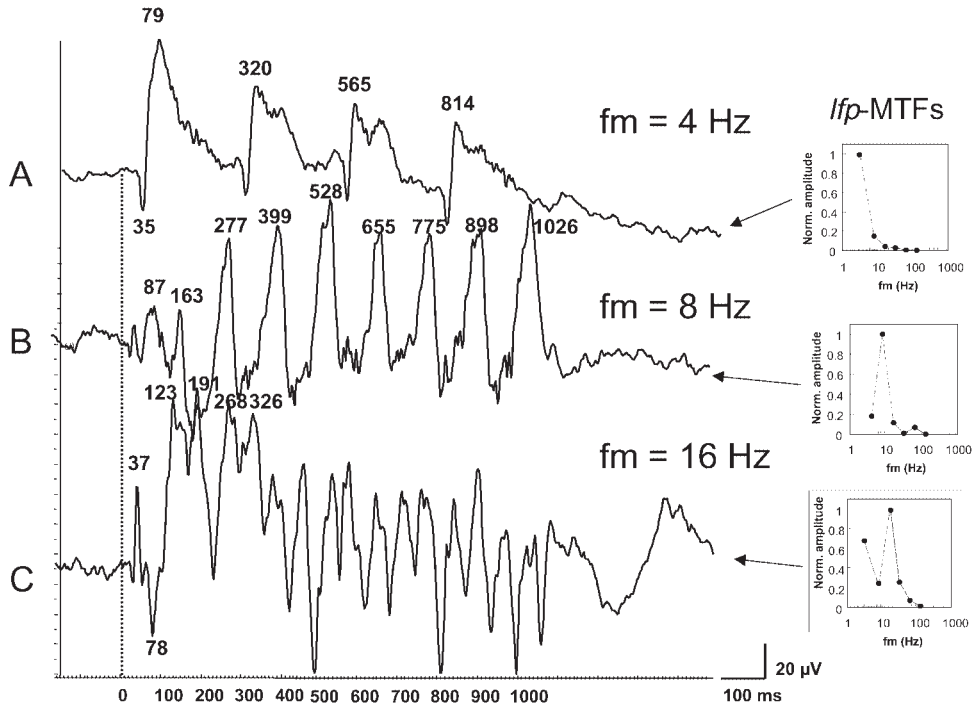

Figure 3. Left panel: auditory evoked potentials (AEPs) recorded from three HG sites (A, B or C). These AEP responses were recorded in the left SAC (A, top graph), right PAC (B, middle graph) and left PAC (C, bottom graph). The ordinate shows the amplitude of the evoked response in μV and the abscissa shows time in milliseconds. The stimulus modulation frequency *fm* is 4 Hz (upper graph), 8 Hz (middle graph), or 16 Hz (lower graph). Right panels: 'Local field potential' modulation transfer functions (*lfp*-MTFs) computed from average AEPs recorded from those sites. *lfp*-MTFs show the magnitude of the frequency components of the AEP response as a function of stimulus AM frequency *fm*. For a given subject and a given electrode, each magnitude is divided by the maximum magnitude value observed across electrode contacts. Therefore, each *lfp*-MTF shows the normalized magnitude of the response evoked by AM (ranging from 0 to 1) as a function of stimulus AM frequency (in Hz). The present *lfp*-MTFs show best synchronization to AM for *fm* = 4 Hz in A, *fm* = 8 Hz in B and *fm* = 4 and 16 Hz in C.

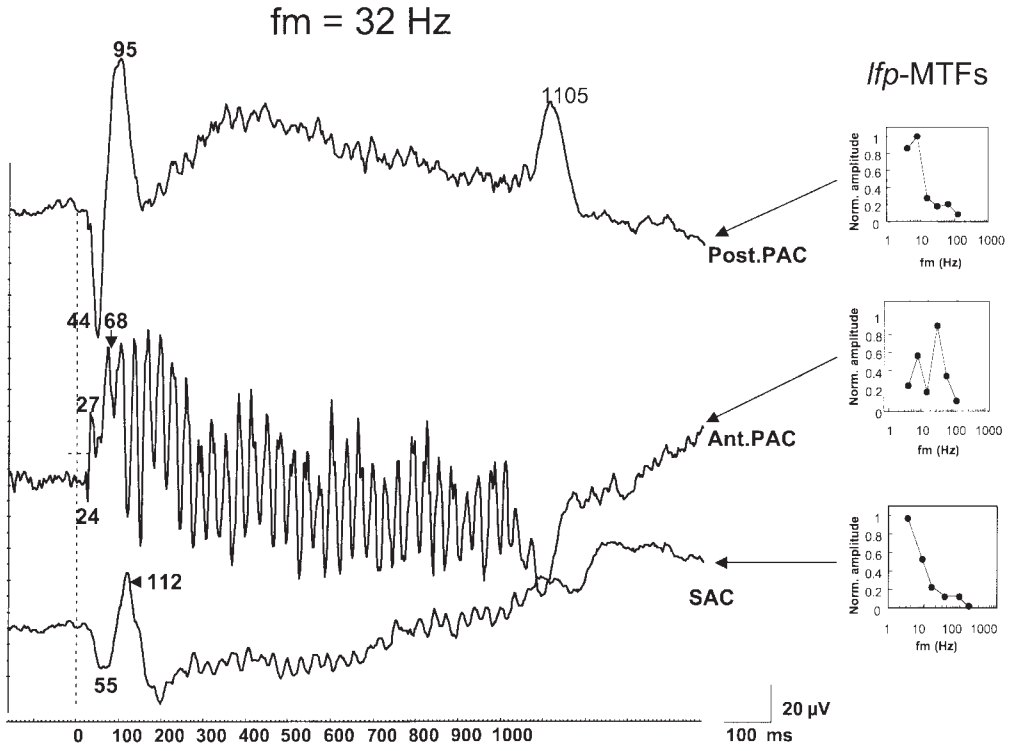

Figure 4. Left panel: AEPs recorded from PAC (posterior and anterior parts of PAC: Post PAC and Ant PAC) and SAC sites in the same patient. The ordinate shows the amplitude of the evoked response in µV and the abscissa shows time in milliseconds. For each graph, the stimulus modulation frequency *fm* is 32 Hz. Right panels: *lfp*-MTFs computed from average AEPs recorded from those three sites. Each *lfp*-MTF shows the normalized magnitude of the response evoked by AM (ranging from 0 to 1) as a function of stimulus AM frequency *fm* (in Hz). Here, the stimulus modulation frequency *fm* is 32 Hz. Note the large amplitude of phase-locked responses in the anterior part of PAC and the absence of phase-locked responses to the AM of 32 Hz in the posterior part of PAC and SAC. *lfp*-MTFs corresponding to these recording sites show a best modulation frequency (BMF) at 8 Hz in the posterior part of PAC, a BMF at 32 Hz in the anterior part of PAC and a corner modulation frequency (CMF) at 4 Hz in SAC.

lowest modulation frequency used in this study (4 Hz). Some *lfp*-MTFs show clear tuning to BMFs ranging from 8 to 16 Hz, resulting in a bandpass shape (second row). Interestingly, two-peak *lfp*-MTFs can be observed, although this profile appears in 4% of the total number of recording sites only. In the right PAC (third row), these two-peak *lfp*-MTFs show BMFs of 8 and 32 Hz. However, the two peaks of *lfp*-MTFs do not systematically occur at these AM frequencies: two-peak *lfp*-MTFs with CMFs or BMFs of 4 and 8 Hz are also observed in the left PAC, left SAC and the left and right BA 22, and two-peak *lfp*-MTFs with CMFs or BMFs of 4 or 16 Hz are observed in the left and right PAC. Finally, a limited number of cortical sites distributed across auditory areas appear insensitive to AM (bottom row), at least for the range of modulation frequencies under study (4–128 Hz). These sites were responsive to other stimuli (noise bursts, etc.) and showed on/off responses.

Anatomical Distribution of AM Responses Within the Left and Right Auditory Cortices

For each auditory area, Figure 6 shows the amplitude of the AEP's main spectral peak averaged across leads within each auditory area as a function of AM frequency. Overall, Figure 6 shows that the amplitude of the AEP's main spectral peak is greater between 4 and 16 Hz and decreases beyond 16 Hz. Residual activity at the highest rates (32–128 Hz) is observed in PAC. This visual impression is confirmed by *post hoc* statistical analyses (Wilcoxon tests) showing that the amplitude of the AEP at the highest rates (32–128 Hz) is significantly lower than the amplitude at 4, 8 and 16 Hz in left and right PAC ($P < 0.001$), in left ($P < 0.001$) and right SAC ($P < 0.03$), in left ($P > 0.001$) and right Post T1 ($P < 0.005$) and BA 22 ($P < 0.006$).

For each modulation frequency, no difference is observed between the left and right PAC. However, at 4 Hz, significant differences in amplitude are observed between the left and right SAC (Mann–Whitney, $U = 72$, $P < 0.005$) and the left and right post T1 (Mann–Whitney, $U = 53$, $P < 0.004$). Interestingly, these cortical areas appear more sensitive to a 4 Hz AM in the left hemisphere than in the right one. Statistical analyses also reveal that the difference in amplitude observed in SAC and post T1 at 8 Hz between the left and right hemispheres is not significant ($P > 0.2$).

Figure 7 presents the distribution of CMFs (4 Hz) or BMFs for each auditory area, that is the percentage of contacts showing a maximum at a given AM frequency in the lowpass, bandpass and two-peak *lfp*-MTFs. Overall, the distributions presented here reveal that, both in the left and right auditory cortices, AEPs are mainly synchronized to the lowest AM frequencies of 4 and 8 Hz. Few AEPs show best synchronization to 16 Hz across the auditory areas under study. AEPs showing best synchronization to 32 Hz are only recorded in PAC. Insensitivity to AM is found in <5% of the leads.

The left auditory areas show a similar ability to follow a 4 Hz AM frequency, and synchronization to this frequency is found as frequently in the left and right hemispheres (χ^2 test < 3.84). No significant difference is found between the distributions observed for frequencies of 4 and 8 Hz, except in SAC for which 73% of sites show a CMF of 4 Hz ($\chi^2 = 5.39$, $P < 0.002$). Synchronization to 8 Hz is more frequently observed in the

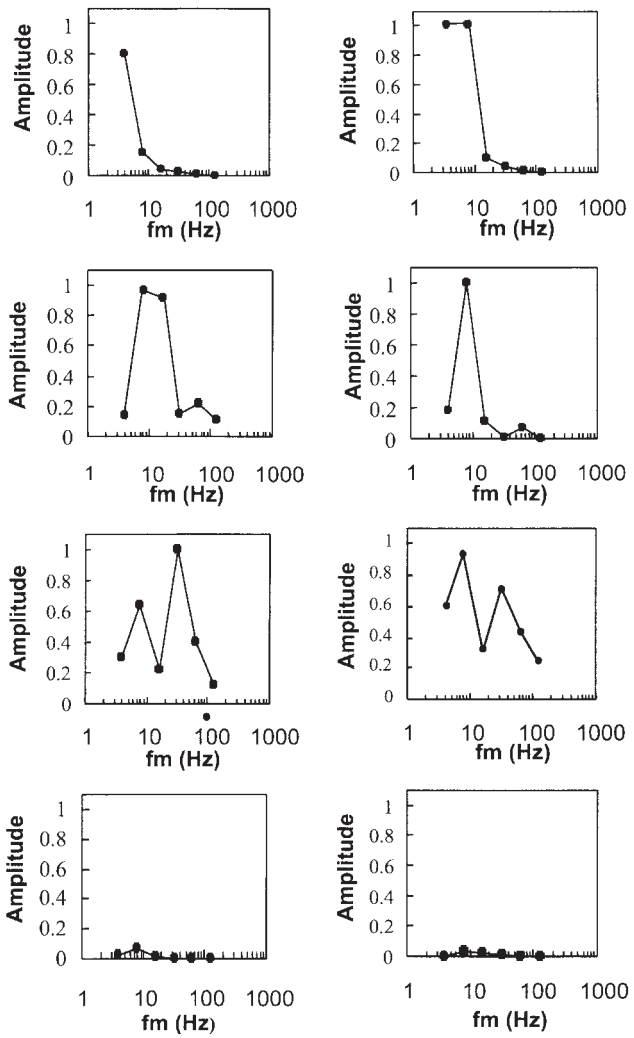

Figure 5. Different types of *lfp*-MTF derived from the amplitude spectra of AEPs. *lfp*-MTFs show the magnitude of the frequency components of the AEP response as a function of stimulus AM frequency. For a given subject and a given electrode, each magnitude is divided by the maximum magnitude value observed across electrode contacts. Therefore, each *lfp*-MTF shows the normalized magnitude of the response evoked by AM (ranging from 0 to 1) as a function of stimulus AM frequency (in Hz). *lfp*-MTFs are either lowpass (top row), bandpass (second row), multi-peak (third row), or flat (bottom row) in shape. The cortical location of each *lfp*-MTF is specified in each panel.

right areas, especially in PAC ($\chi^2 = 21.5$, $P < 0.0001$) and in post T1 compared to SAC ($\chi^2 = 8.73$, $P < 0.01$ and $\chi^2 = 14.3$, $P < 0.001$, respectively) and BA 22 ($\chi^2 = 8.12$, $P < 0.004$; $\chi^2 = 13.7$, $P < 0.0002$). A significant hemispheric difference is observed for this modulation frequency between the left and right PAC ($\chi^2 = 10$, $P < 0.01$) and left and right post T1 ($\chi^2 = 7.8$, $P < 0.01$). Finally, synchronization at 16 Hz is more frequently observed in the left PAC than the right PAC ($\chi^2 = 4.5$, $P < 0.05$).

Finally, the spatial distribution of CMFs and BMFs is investigated in the right and left auditory cortices (Figs 8*A*,*B*, respectively) in two patients (Cases 3 and 20) showing more than one implanted electrode in auditory areas (thus, allowing greater spatial sampling, i.e. 30 recording sites in Case 3 and 11 recording sites in Case 20). Each figure is a map presenting the spectral content of AEPs for each recording site (amplitude being represented by a color code) and the anatomical location of corresponding contacts surperimposed on the MRI. The data are interpolated so as to smooth the pictures. In the right PAC (Case 3, Fig. 8*A*), BMFs of 32 Hz are recorded in the most medial site, BMFs of 16 Hz are recorded in the following lateral lead and BMFs of 8 Hz are recorded in the more lateral and anterior sites. In the left PAC (Case 20; Fig. 8*B*), the anterior part of PAC (T11–T15) is mainly sensitive to a 4 Hz AM frequency and, to a lesser degree, to a 16 Hz AM and the posterior part of PAC (H13, H14) is mainly sensitive to a 16 Hz AM frequency. Overall, these data demonstrate unambiguously the existence of neural sites tuned to low AM frequencies, but do not reveal any consistent and clearly ordered representation for low AM frequencies.

Discussion

Overall, the present data indicate: (i) a selective encoding of AM frequency in the human auditory cortex – at least for AM frequencies below 64 Hz; (ii) a predominant response of cortical auditory areas to the low AM frequencies (4–8 Hz) known to be crucial for speech perception; (iii) differences in temporal resolution across human cortical auditory areas; and finally, (iv) the data do not reveal any spatial mapping of AM frequency within the human auditory cortex; but (v) indicate inter-hemispheric differences in temporal-envelope coding. These results are discussed below.

Selective Encoding of Temporal Envelope Fluctuations in the Human Auditory Cortex

The present results show that, in the human auditory cortex, AM noise evokes phase-locked responses in different auditory areas for a specific range of modulation frequencies (cf. Figs 3 and 4). As specified above, phase-locked responses have been observed in 74% of the recording sites. It is noteworthy that a similar proportion of acoustically driven neurons is found in the awake squirrel monkey by Bieser and Müller-Preuss (1996). Moreover, three types of AM response have been identified with respect to the shape of the *lfp*-MTF, recording sites showing either lowpass, bandpass (i.e. single-peak) or two-peak *lfp*-MTFs (cf. Fig. 5). These three categories may however correspond to two categories only – bandpass and two-peak *lfp*-MTFs – given the fact that modulation frequencies lower than 4 Hz have not been tested. The data also show that CMFs and BMFs range from 4 to 32 Hz. The occurrence of two-peak *lfp*-MTF could be interpreted in two ways. First, it may reveal the existence of strong clusters of specific BMFs in close spatial proximity, but separate (therefore, the two-peak nature results from electrical superposition and is due to the recording configuration). Alternatively, the existence of two peaks may correspond to a feature present in single neurons, with strong local clustering of such a property.

For ~20 years, a number of psychoacoustical studies based on selective-adaptation or masking procedures applied to the AM domain (e.g. Kay and Matthews, 1972; Bacon and Grantham, 1989; Houtgast, 1989; Yost *et al.*, 1989; Dau *et al.*, 1997a,b; Lorenzi *et al.*, 1997; Ewert and Dau, 2000) have suggested the existence of 'modulation channels' or, in other words, some form of tuning of the human auditory system in the AM domain (i.e. in the temporal-envelope domain). According to these psychoacoustical studies, modulation channels broadly tuned to modulation frequencies below ~100 Hz may be organized as an array orthogonal to the tonotopic axis and allow the decomposition of the temporal envelope of

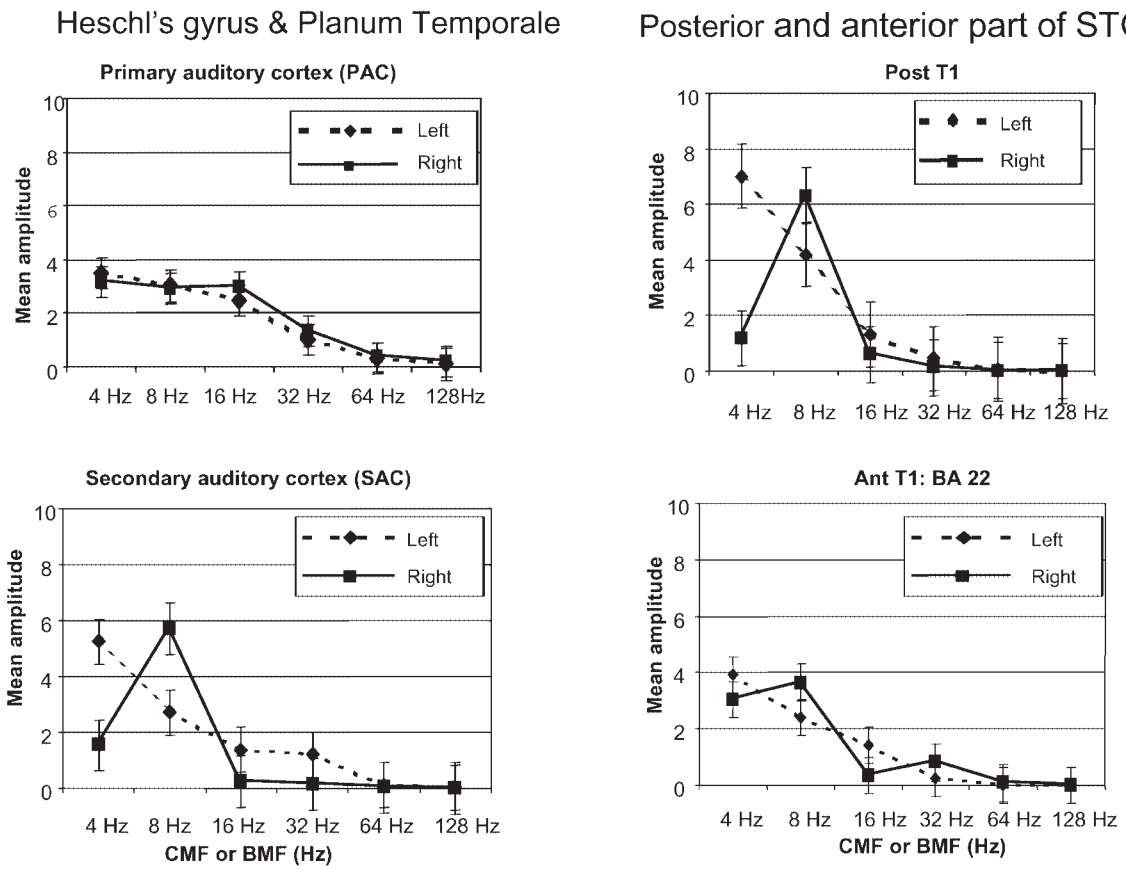

Figure 6. Mean amplitude at CMF or BMF in each cortical auditory area (PAC, SAC, Post T1 and BA 22) of the left (L) and right (R) hemisphere. Each plot shows the amplitude of the AEP's main spectral peak [i.e. amplitude in μV at CMF (4 Hz) or BMF in the corresponding *lfp*-MTF] averaged across leads for a given auditory area, as a function of the AM frequency of the main spectral peak.

incoming sounds in each audio-frequency channel. However, other psychoacoustical and modelling studies refute the notion of modulation channel and suggest that non-selective temporal mechanisms may also be able to account for the psychoacoustical data on AM perception (e.g. Strickland and Viemeister, 1996). The present SEEG study reveals the existence of neural sites tuned to specific AM frequencies in the human auditory cortex. It therefore provides strong physiological evidence supporting the modulation filterbank approach and suggests that the human central auditory system decomposes the envelope of sounds (for instance, speech sounds) into its AM components.

Prominent Response of Cortical Auditory Areas to Low Modulation Frequencies

The results presented in Figures 6 and 7 show that AM frequencies ranging from 4 to 32 Hz evoke following transient responses in the auditory cortex and that the latter is clearly more sensitive to the lowest AM frequencies (4–8 Hz). These results are consistent with those obtained in previous electrophysiological and fMRI studies carried out in animals and humans, showing that BMFs in most cortical auditory fields range between 2 and 30 Hz (e.g. Schreiner and Urbas, 1986, 1988; Eggermont, 1998; Giraud *et al.*, 2000). These results are also in line with speech perception, brain imaging and neuropsychological studies suggesting that the match between the speech rate (2–16 Hz) and the modulation-following capacities of the human auditory cortex (estimated to 4–32 Hz in the present study) is a prerequisite for speech intelligibility (e.g. Hescot *et al.*, 2000; Lorenzi *et al.*, 2000; Ahissar *et al.*, 2001). Moreover, it is interesting to note that, according to neuropsychological studies, the capacity to follow these low AM rates is degraded in brain-damaged patients showing a deficit in music perception (e.g. Griffiths *et al.*, 2000).

Unlike previous animal studies (e.g. Steinschneider *et al.*, 1980; Schreiner and Urbas, 1986, 1988), little or no response to AM rates >32 Hz was obtained in the present SEEG study. It must be pointed out that the SEEG technique shows some intrinsic limitations that might have obscured responses to such high AM rates: given the size of electrode contacts used in the present study (0.8 mm diameter, 2 mm length), it is conceivable that responses to AM rates greater than 32 or 64 Hz could not be observed.

Differences in Temporal Resolution across Human Auditory Cortical Areas

The results presented in Figures 6 and 7 show that responses to AM sounds differ across the different auditory areas. Overall, these results show that AEPs recorded in most cortical areas are mainly synchronized to the lowest AM frequencies of 4 and 8 Hz and, to a lesser extent, to 16 Hz. However, AEPs showing best synchronization to 32 Hz appear only in PAC, suggesting that temporal resolution is higher in the primary auditory area. Similar differences in the organization of temporal resolution

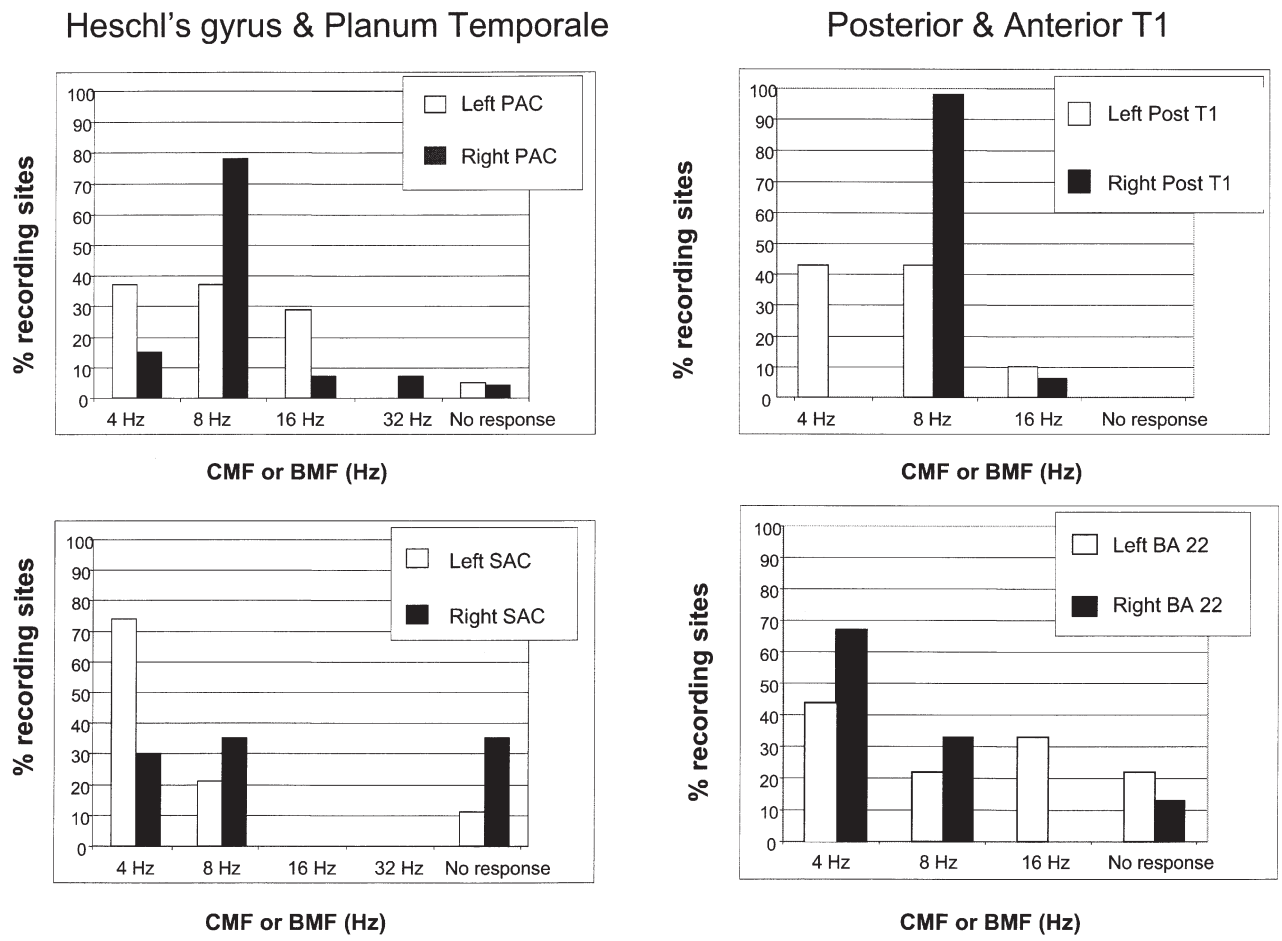

Figure 7. Distribution of CMFs and BMFs expressed in terms of percentage of number of sites, for each auditory area of the left and right hemisphere.

between cortical auditory areas – and especially between primary and non primary auditory fields – have been reported for the cat and squirrel monkey (Schreiner and Urbas, 1986, 1988; Bieser and Müller-Preuss, 1996; Eggermont, 1998). In these (single-neuron) electrophysiological studies, synchronous responses to high or moderately high frequencies (14–32 Hz) were found in neurons belonging to PAC (called AI in animals), whereas neurons in most cortical fields were generally tuned to lower frequencies. The present data also show that the strongest responses to 4 and 8 Hz are recorded in SAC and post T1. This is in good agreement with an fMRI study on human subjects (Giraud *et al.*, 2000), which shows that regions lateral and posterior to HG are more sensitive to the low frequencies of 4 and 8 Hz. The differences in temporal resolution across cortical areas reported in the present SEEG study therefore provide a physiological foundation for claims of functional specialization of auditory cortical areas based on population measures (such as fMRI).

No Spatial Mapping of Modulation Frequency within the Human Auditory Cortex

Two previous studies cited above report the existence of a spatial mapping of high AM frequencies (>100–200 Hz) in the auditory cortex. In contrast with these studies, the present results do not demonstrate the existence of spatial mapping for low AM frequencies (<100 Hz) in the human primary auditory cortex. This is relatively surprising knowing that low AM rates are crucial for speech perception and that important sensory dimensions (such as audio-frequency) are generally mapped in the brain. Given the low spatial resolution of the present recording device and methodology and given the complex nature of other potential topographical principles such as binaurality, it is not really unexpected that AM topography is not immediately evident. However, this negative result is in line with the general conclusions of the fMRI study conducted by Giraud *et al.* (2000). This fMRI study clearly shows distinct clusters of voxels responding selectively to specific AM frequencies, but fails to observe any clear spatial gradient for AM frequencies belonging to the range used in the present study (4–128 Hz).

Inter-hemispheric Differences

The results of a previous study indicate that AEPs recorded in the left human auditory cortex are related to the temporal structure of sounds, in so far as voiced and voiceless consonants (e.g. /ba/,/pa/) appear to be processed differently in left HG. This processing seems to be related to the acoustic rather than to the phonetic features of speech sounds, because identical time-locked responses are recorded for speech and non-speech sounds showing the same time course (Liégeois-Chauvel *et al.*, 1999). In the present study, the use of AM noises showing a flat power spectrum ensures that the observed brain responses do reflect specific temporal processing. However, in contrast to the results of Liégeois-Chauvel *et al.* (1999), we find

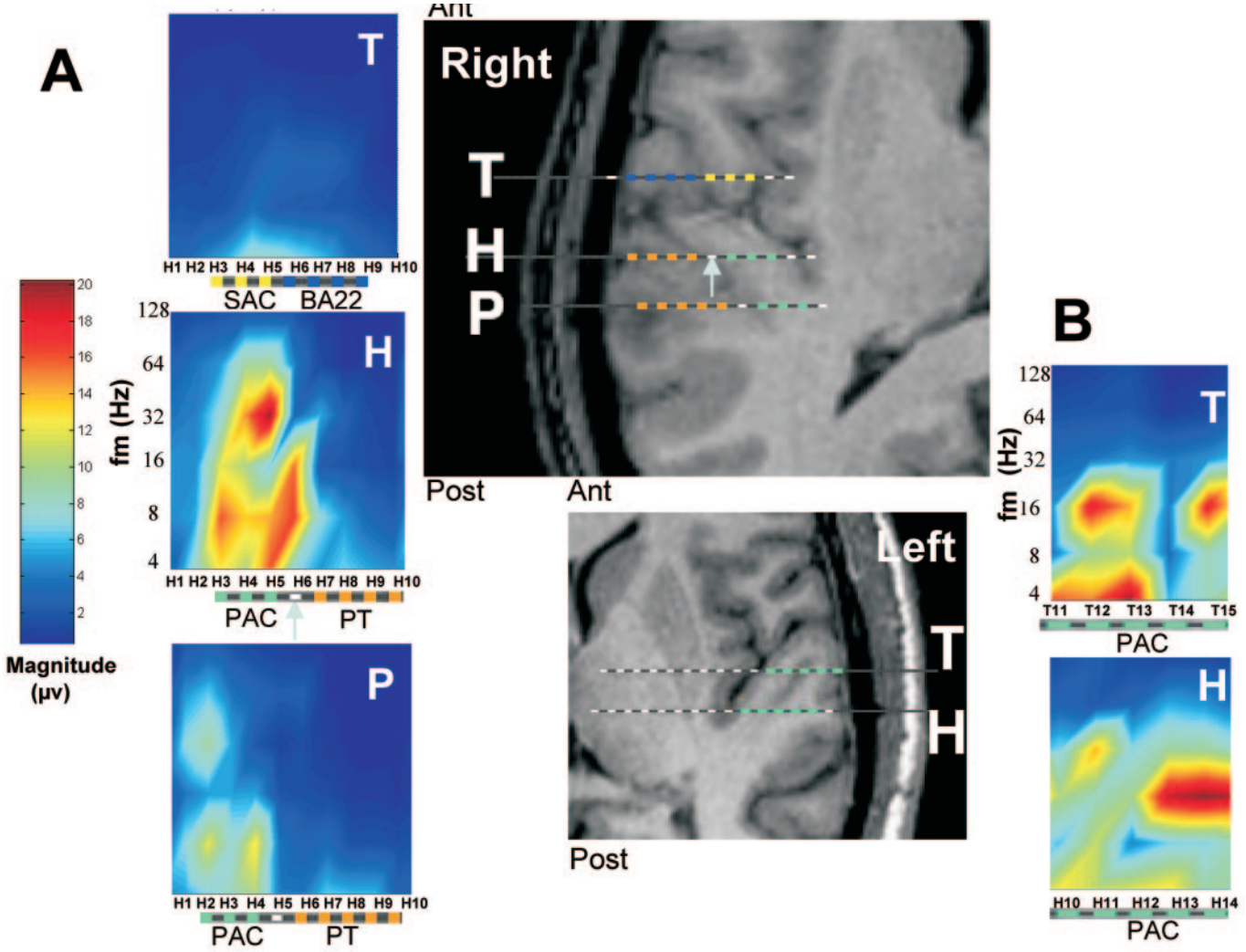

Figure 8. (*A*, *B*) Spatial distribution of the responses to AM in the right (*A*) or left (*B*) auditory cortices of two patients. Each blue, yellow, red, or green line indicates which auditory region is recorded and its anatomical location on the electrode superimposed on the MRI. Spectral magnitude is represented by a color code. Note that a single electrode can record cortical activity from different areas. (*A*) Note the spatial segregation of CMFs or BMFs within PAC: BMFs of 8 Hz are observed in H3, BMFs of 32 Hz are observed in H4 and CMFs or BMFs of 4, 8 and 16 Hz are observed in H5 (these leads are located in the anterior PAC). The green arrow indicates that H6 passes through a sulcus between HG and PT. (*B*) BMFs of 16 Hz are observed in H13 and H14, while CMFs of 4 Hz are observed in T11, T12 and T13.

similar following evoked responses to AM noises in both hemispheres (e.g. Fig. 6).

Nevertheless, the different cortical areas investigated in the present study show clear differences in their capacity to follow slow temporal modulations. Figure 7 shows that the left PAC and post T1 areas are equally sensitive to 4 and 8 Hz AM, while homologous areas in the right hemisphere respond mainly to a 8 Hz AM. A similar (but striking) difference in sensitivity to low AM sounds (4–8 Hz) is also found between left and right SAC, suggesting that these areas may have a specific role in temporal envelope coding. Overall, the left areas cited above encode accurately slow AM frequencies of 4 and 8 Hz, whereas the right homologues show better ability to encode a 8 Hz AM frequency. AM frequencies crucial for speech intelligibility range from 4 to 16 Hz (e.g. Drullman *et al.*, 1994a,b; Shannon *et al.*, 1995). According to our data, both left and right cortical areas such as PAC, SAC and posterior T1 should therefore play a role in speech envelope encoding.

Notes

We would like to thank P. Marquis for assisting us in data collection, B. Gourevitch for performing spatial maps and G. Canévet for useful comments on a previous version of this paper. We would also like to thank two anonymous reviewers for helpful comments on an earlier version of this manuscript. This study was supported by the Cognitique program (MENRT), Medical Research Foundation (MRF) and Institut Universitaire de France.

Address correspondence to C. Liégeois-Chauvel, INSERM EMI-U 9926, Laboratoire de Neurophysiologie et Neuropsychologie, Faculté de Médecine, 27 Bd Jean Moulin, 13005 Marseille, France. Email: Catherine.liegeois@medecine.univ-mrs.fr.

References

Ahissar E, Nagarajan S, Ahissar M, Protopapas A, Mahncke H, Merzenich MM (2001) Speech comprehension is correlated with temporal response patterns recorded from auditory cortex. Proc Natl Acad Sci USA 98:13367–13372.

Bancaud J, Talairach J, Bonis A, Schaub C, Szikla G, More P, Bordas-Ferrer M (1965) La stéréoélectroencéphalographie dans

l'épilepsie: informations neurophysiopathologiques apportées par l'investigation fonctionnelle stéréotaxique. Paris: Masson.
Bacon SP, Grantham DW (1989) Modulation masking: effects of modulation frequency, depth, and phase. J Acoust Soc Am 85:2575–2580.
Bieser A, Müller-Preuss P (1996) Auditory responsive cortex in the squirrel monkey: neural responses to amplitude-modulated sounds. Exp Brain Res 108:273–284.
Dau T, Kollmeier B, Kohlrausch A (1997a) Modeling auditory processing of amplitude modulation: I., Modulation detection and masking with narrow-band carriers. J Acoust Soc Am 102:2892–2905.
Dau T, Kollmeier B, Kohlrausch A (1997b) Modeling auditory processing of amplitude modulation: II., Spectral and temporal integration in modulation detection. J Acoust Soc Am 102:2906–2919.
Drullman R, Festen JM, Plomp R (1994a) Effect of temporal envelope smearing on speech reception. J Acoust Soc Am 95:1053–1064.
Drullman R, Festen JM, Plomp R (1994b) Effect of reducing slow temporal modulations on speech reception. J Acoust Soc Am 95:2670–2680.
Eggermont JJ (1994) Temporal modulation transfer functions for AM and FM stimuli in cat auditory cortex. Effects of carrier type, modulating waveform and intensity. Hearing Res 74:51–66.
Eggermont JJ (1998) Representation of spectral and temporal sound features in three cortical fields of the cat. Similarities outweigh differences. J Neurophysiol 80:2743–2764.
Ewert SD, Dau T (2000) Characterising frequency selectivity for envelope fluctuations. J Acoust Soc Am 108:1181–1196.
Frisina RD (2001) Subcortical neural coding mechanisms for auditory temporal processing. Hearing Res 158:1–27.
Giraud AL, Lorenzi C, Ashburner J, Wable J, Johnsrude I, Frackowiak R, Kleinschmidt A (2000) Representation of the temporal envelope of sounds in the human brain. J Neurophysiol 84:1588–1598.
Griffiths TD, Penhune V, Peretz I, Dean JL, Patterson RD, Green GG (2000) Frontal processing and auditory perception. Neuroreport 7:919–922.
Hescot F, Lorenzi C, Debruille X, Camus JF (2000) Amplitude-modulation detection for broadband noise in a single listener with left-hemisphere damage. Br J Audiol 34:341–351.
Houtgast T (1989) Frequency selectivity in the amplitude-modulation domain. J Acoust Soc Am 85:1676–1680.
Kaltwasser MT (1990) Acoustic signaling in the black rat (*Rattus rattus*). J Comp Psychol 104:227–232.
Kay RH, Matthews DR (1972) On the existence in human auditory pathways of channels selectively tuned to the modulation present in frequency-modulated tones. J Physiol 225:657–677.
Langner G (1992) Periodicity coding in the auditory system. Hearing Res 60:115–142.
Langner G, Sams M, Heil P, Schulze H (1997) Frequency and periodicity are represented in orthogonal maps in the human auditory cortex: evidence from magnetoencephalography. J Comp Physiol 181:665–676.
Liégeois-Chauvel C, Musolino A, Chauvel P (1991) Localization of the primary auditory area in man. Brain 114: 139–153.
Liégeois-Chauvel C, Musolino A, Badier JM, Marquis P, Chauvel P (1994) Evoked potentials recorded from the auditory cortex in man: evaluation and topography of the middle latency components. Electroencephalogr Clin Neurophysiol 92:204–214.
Liégeois-Chauvel C, de Graaf JB, Laguitton V, Chauvel P (1999) Specialization of left auditory cortex for speech perception in man depends on temporal coding. Cereb Cortex 9:484–496.
Lorenzi C, Micheyl C, Berthommier F, Portalier S (1997) Modulation masking in listeners with sensorineural hearing loss. J Speech Lang Hearing Res 40:200–207.
Lorenzi C, Dumont A, Füllgrabe C (2000) Use of temporal envelope cues by developmental dyslexics. J Speech Lang Hearing Res 43:1367–1379.
Mangin JF, Frouin V, Boc I, Régis J, Lopez-Knohe J (1995) From 3D magnetic resonance images to structural representations of the cortex topography using typology preserving deformations. J Math Imaging Vis 5:267–318.
Rees A, Green GGR, Kay RH (1986) Steady-state evoked responses to sinusoidally amplitude-modulated sounds recorded in man. Hearing Res 23:123–133.
Rocheron I, Lorenzi C, Füllgrabe C, Legros V, Dumont A (2002) Temporal envelope perception in dyslexic children. Neuroreport 13:1683–1687.
Roß B, Borgmann C, Draganova R, Roberts LE, Pantev C (2000) A high-precision magnetoencephalographic study of human steady-state responses to amplitude-modulated tones. J Acoust Soc Am 108:679–691.
Schreiner CE, Urbas JV (1986) Representation of amplitude modulation in the auditory cortex of the cat. I. The anterior auditory field (AAF). Hearing Res 21:227–241.
Schreiner CE, Urbas JV (1988) Representation of amplitude modulation in the auditory cortex of the cat. II. Comparison between cortical fields. Hearing Res 32:49–64.
Schulze H, Langner G (1997) Periodicity coding in the primary auditory cortex of the Mongolian gerbil (*Meriones unguiclatus*): two different coding strategies for pitch and rhythm? J Comp Physiol 181:651–663.
Schulze H, Hess A, Ohl F, Scheich H (2002) Superposition of horseshoe-like periodicity and linear tonotopic maps in auditory cortex of the mongolian gerbil. Eur J Neurosci 15:1077–1084.
Shannon RV, Zeng F, Kamath V, Wygonski J, Ekelid M (1995) Speech recognition with primarily temporal cues. Science 270:303–304.
Smith ZM, Delgutte B, Oxenham AJ (2002) Chimaeric sounds reveal dichotomies in auditory perception. Nature 416:87–90.
Steinschneider M, Arezzo J, Vaughan HG Jr (1980) Phase-locked cortical responses to a human speech sound and low-frequency tones in the monkey. Brain Res 198:75–84.
Steeneken HJM, Houtgast T (1980) A physical method for measuring speech-transmission quality. J Acoust Soc Am 67:318–326.
Strickland EA, Viemeister NF (1996) Cues for discrimination of envelopes. J Acoust Soc Am 99:3638–3646.
Szikla G, Bouvier G, Hori T, Petrov V (1977) Angiography of the human brain cortex. Atlas of vascular patterns and stereotactic cortical localization. Berlin: Springer.
Talairach J, Tournoux P (1988) Co-planar stereotaxic atlas of the human brain. Three-dimensional proportional system: an approach to cerebral imaging. Stuttgart: Georg Thieme.
Talairach J, Bancaud J, Szikla G, Bonis A, Geier S, Vedenne C (1974) Approche nouvelle de la neurochirurgie de l'épilepsie. Methodologie stéréotaxique et résultats thérapeutiques. Neurochirurgie 20:1–240.
Viemeister NF (1979) Temporal modulation transfer functions based upon modulation thresholds. J Acoust Soc Am 66:1364–1380.
Witton C, Stein JF, Stoodley CJ, Rosner BS, Talcott JB (2002) Separate influences of acoustic AM and FM sensitivity on the phonological decoding skills of impaired and normal readers. J Cogn Neurosci 15:866–874.
Yost WA, Sheft S, Opie J (1989) Modulation interference in detection and discrimination of amplitude-modulation. J Acoust Soc Am 86:2138–2147.